in eq 4 but remains on the catalyst surface.

Basu et al. has stated that a linear correlation between the loss of OH intensity in the isolated OH and the gain in integrated intensity in the associated OH species does not *seem* to exist, which is not in perfect accordance with the scheme shown in Figure 10. Accordingly, further studies concerning the reaction mechanism are definitely required, because reactions of small metal clusters in supported catalysts with adsorbates may play a crucial role in heterogeneous catalysis.

Registry No. Ru, 7440-18-8; MgO, 1309-48-4; TiO_2, 13463-67-7; CO, 630-08-0.

Slow Dissociations of Thiophenol Molecular Ion. Study by TRPD and TPIMS

James D. Faulk,† Robert C. Dunbar,*,† and Chava Lifshitz*,‡

Contribution from the Chemistry Department, Case Western Reserve University, Cleveland, Ohio 44106, and Department of Physical Chemistry and The Fritz Haber Research Center for Molecular Dynamics, The Hebrew University of Jerusalem, Jerusalem 91904, Israel.
Received March 12, 1990

Abstract: Dissociation of thiophenol molecular ion to yield competitive product ions at m/z 84 ($C_4H_4S^+$) and 66 ($C_5H_6^+$) was studied by several techniques. Time-resolved photodissociation at 308 nm (4.20 eV ion internal energy) in the ICR ion trap gave rate constants of 1.3×10^5 s^{-1} for m/z 84 formation and 8×10^4 s^{-1} for m/z 66 formation, and at 355 nm (3.66 eV ion internal energy) it gave 2.8×10^3 s^{-1} for m/z 84 formation, with m/z 66 not observed at this wavelength. Time-resolved photoionization mass spectrometry at 800 μs trapping time gave thresholds of 2.9 eV for m/z 84 formation and 3.2 eV for m/z 66 formation; the photoionization efficiency curves cross at approximately 4 eV internal energy so that m/z 66 is more abundant at energies above this; at 20-μs trapping a kinetic shift of approximately 0.2 eV was observed relative to 800-μs trapping. MIKES spectra indicated a low average kinetic energy release for metastable ion decomposition, $\langle T \rangle = 52 \pm 5$ meV, for m/z 66, and a higher kinetic energy release, $\langle T \rangle = 151 \pm 5$ meV, for m/z 84. RRKM modeling of these dissociations was successful, using a very loose transition state ($\Delta S^{\ddagger}(1000\ K) = 14$ eu) and a critical energy of 3.2 eV for m/z 66 formation, a tighter transition state ($\Delta S^{\ddagger}(1000\ K) = 2.74$ eu) and a critical energy of 2.9 eV for m/z 84 formation. With use of TRPD as an ion-thermometric tool, collisional cooling of hot thiophenol ions by collisions with neutral thiophenol was observed and a collisional cooling rate constant of 4×10^{-10} cm^3·molecule^{-1}·s^{-1} was measured.

Introduction

Because charged molecules are easy to manipulate and detect, the study of unimolecular dissociation kinetics has received much impetus from ion dissociations studied in various kinds of mass spectrometers. The most clear-cut and satisfactory experiments of this kind have taken advantage of the ability of photons to deposit precisely known increments of energy, affording to various photoionization and photodissociation experiments the advantage of excellent knowledge of the internal energy of the fragmenting molecule.

Recent advances in studying dissociation kinetics by both photoionization and photodissociation have opened up ways of observing unimolecular dissociations with very low rates, having dissociation time constants of several milliseconds or longer. The time-resolved photoionization mass spectrometry (TPIMS) experiment in the quadrupole ion trap[1] and the time-resolved photodissociation (TRPD) experiment in the ion cyclotron resonance (ICR) ion trap[2] are two such techniques that are finding application to a variety of slow-dissociation systems.

The dissociation of thiophenol ion in the region of 3.5–4.5 eV internal energy is a slow dissociation about which little quantitative kinetic information has been available, and the application of these two techniques has provided the first rate values for this system. In the internal energy regime of interest here, the ion dissociates competitively to two products according to

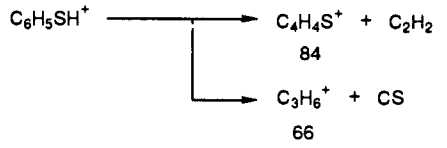

Initial TRPD observations[3] of the rate of m/z 66 production from thiophenol ion photodissociation at 308 nm indicated a unimolecular rate constant near 10^5 s^{-1}. This rate was strikingly faster than the approximately 1×10^3 s^{-1} predicted from reasonable RRKM modeling of the process. A tight transition state was assumed in this initial modeling of this system, considered to be almost surely involved in such a rearrangement fragmentation.

This unexpected result inspired a more extensive examination of the system, to investigate whether (a) the initial TRPD observations were flawed, (b) the thermochemically derived activation energy of 3.2 eV used in the modeling was too high, (c) the assumption of a tight transition state should be reconsidered, or (d) RRKM theory (which involves statistical or quasiequilibrium theory assumptions) is violated in this case. Experiments with the TRPD and TPIMS techniques, along with auxiliary work with Fourier-transform mass spectrometry, two-photon photodissociation, and MIKES, have been used to characterize the dissociation channels yielding both m/z 66 and 84, leading finally to a satisfactory picture of this system in the slow-dissociation regime.

Experimental Section

The ICR–TRPD experiments were carried out as has been described in detail in previous publications,[2] using the phase-sensitive-detection ICR

† Case Western Reserve University.
‡ Archie and Marjorie Sherman Professor of Chemistry. The Hebrew University of Jerusalem.

(1) (a) Lifshitz, C.; Goldenberg, M.; Malinovich, Y.; Peres, M. *Org. Mass Spectrum.* **1982**, *17*, 453. (b) Malinovich, Y.; Arakawa, R.; Haase, G.; Lifshitz, C. *J. Phys. Chem.* **1985**, *89*, 2253. (c) Ziesel, J. P.; Lifshitz, C. *Chem. Phys.* **1987**, *177*, 227. (d) Ohmichi, N.; Malinovich, Y.; Ziesel, J. P.; Lifshitz, C. *J. Phys. Chem.* **1989**, *93*, 2491. (e) Lifshitz, C.; Ohmichi, N. *J. Phys. Chem.* **1989**, *93*, 6329.

(2) (a) Dunbar, R. C. *J. Phys. Chem.* **1987**, *91*, 2801. (b) So, H. Y.; Dunbar R. C. *J. Am. Chem. Soc.* **1988**, *110*, 3080. (c) Dunbar, R. C. *J. Phys. Chem.* In press. (d) Dunbar, R. C. *J. Am. Chem. Soc.* **1989**, *111*, 5572.

(3) Faulk, J. D.; Dunbar, R. C. Proceedings of the 37th ASMS Conference on Mass Spectrometry and Allied Topics, Miami Beach, FL, May 21–26, 1989, p 254.

(4) Faulk, J. D.; Dunbar, R. C. *J. Phys. Chem.* In press.

(5) Asamoto, B.; Dunbar, R. C. *Chem. Phys. Lett.* **1987**, *139*, 225.

0002-7863/90/1512-7893$02.50/0

spectrometer. Electron impact ionization at a nominal electron energy of 12 eV was used to produce parent ions. A thermalization time of 1–2 s was used between the ionization pulse and the laser pulse; as discussed below in the thermalization studies, pressures of neutral thiophenol varied from 5×10^{-8} to 1×10^{-6} Torr. Following the laser pulse, and following the variable delay, an rf excite pulse of 12 μs duration and 50 V p-p was applied at the daughter ion frequency, followed by transient acquisition for 2 ms. In a typical experiment, the delay time between laser and detection was swept over about 40 values, and 50–100 such sweeps were accumulated and averaged to give the TRPD spectrum.

A Lumonics excimer laser was used at 308 nm, giving a pulse energy of a few millijoules, which was focused to a spot diameter of a few millimeters at the ICR cell. A similar spot at 355 nm was produced by a Lumonics HY-1200 Nd/YAG laser with frequency tripler. Pulses from both lasers have a duration of about 10 ns, which is very short compared with the dissociation and detection time scales.

The Fourier-transform photodissociation mass spectrum was taken on an FT-ICR spectrometer with an IonSpec Fourier-transform data system. The ions were not thoroughly thermalized, with a pulse of light at 308 nm being delivered 100 ms after the electron beam pulse at a pressure of 1.5×10^{-7} Torr.

The method of time-resolved photoionization mass spectrometry (TPIMS) has been described in detail.[1] Photoionization is induced by a pulsed vacuum-ultraviolet light source, a Hinteregger discharge in hydrogen producing the many-line spectrum. Photoions are trapped in a cylindrical ion trap (CIT).[1c] They are ejected into a quadrupole mass filter by a drawout pulse, following a variable delay time. Ions can be stored from microseconds to milliseconds.

The radio frequency of the potential applied to the cylindrical barrel electrode of the CIT is 0.5 MHz ($\omega/2\pi$). The rf voltage chosen for the experiments is at the crossing point of the parent–daughter stability curves,[1b] ensuring equal trapping efficiency. No DC bias was applied to the barrel electrode of the CIT.

The effective wavelength resolution employed is 5.0 Å. This corresponds to an energy resolution near the fragmentation onset of thiophenol, using VUV photoionization, of ≃0.05 eV.

MS/MS measurements were performed on a VG ZAB-2F double-focussing mass spectrometer of reversed geometry. The metastable fragmentations were studied by mass-analyzed ion kinetic energy spectroscopy (MIKES). The magnetic field was set to select the ions of desired m/z value under investigation; ionic products of their decompositions in the second field-free region (2-FFR) between the magnetic and electrostatic analyzers were detected by scanning the electric-sector potential under conditions of good energy resolution with the energy-resolving β-slit partially closed. There is a distribution of sampled rate coefficients with a maximum at $\sim 10^5$ s^{-1}. Collisional activation (CA) spectra were obtained by using He as the collision gas on 8-keV ions. The pressure in the collision cell, in the 2-FFR of the ZAB, was adjusted for CA spectra such that the primary ion beam intensity fell by not more than 30% of its original intensity. The pressure rose from the background level of $\leq 3.8 \times 10^{-9}$ Torr to $\sim 1.5 \times 10^{-7}$ Torr upon the introduction of He.

Results

The principal results are the dissociation rates into each of the two principal products as a function of internal energy of the parent and the kinetic energy release for each of the two products. The kinetic energy release (KER) values come from the MIKES spectra (Hebrew University). Two independent experiments lead to dissociation rates as a function of parent ion internal energy (rate-energy curves): the TRPD experiment (CWRU), and the TPIMS experiment (Hebrew University). The two different experiments give concordant rate–energy curves, allowing high confidence in the results.

Time-Resolved Photodissociation. In the ICR–TRPD experiment,[2] parent ions are formed by electron impact, thermalized, and photoexcited by a monochromatic pulsed laser. The appearance of daughter ions is plotted as a function of delay after the laser pulse, using the fast ICR detection capabilities of the ICR instrument. Since absorption of a photon gives a parent ion of precisely known internal energy (within the spread of initial thermal energies), each TRPD curve gives a single, well-defined point on the rate–energy curve.

There is an important point to remember when dissociation branches into two or more significant competing product channels, as is the case for thiophenol ion photodissociation at 308 nm. At first glance one would expect the shapes of the appearance curves for the two product ions to reflect the unimolecular rate constants

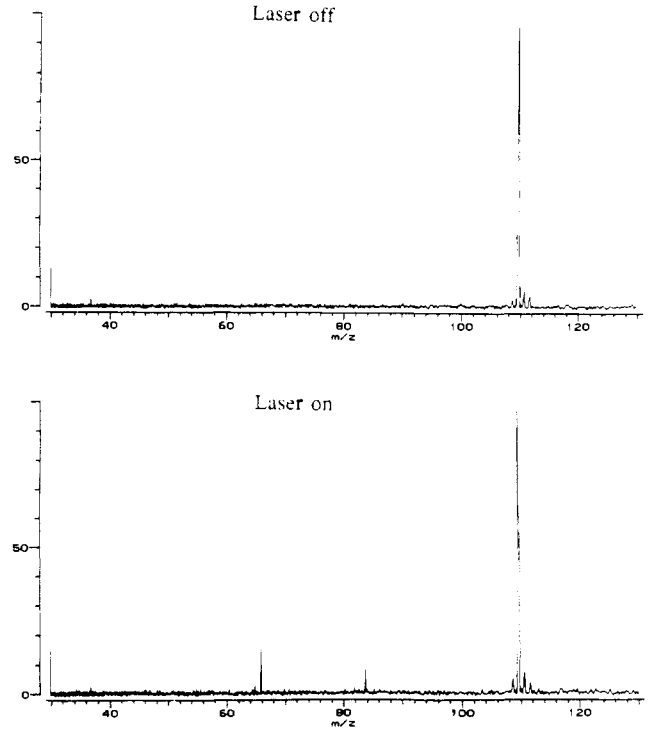

Figure 1. Photodissociation mass spectrum for thiophenol ion photodissociation at 308 nm in the FTMS ion trap.

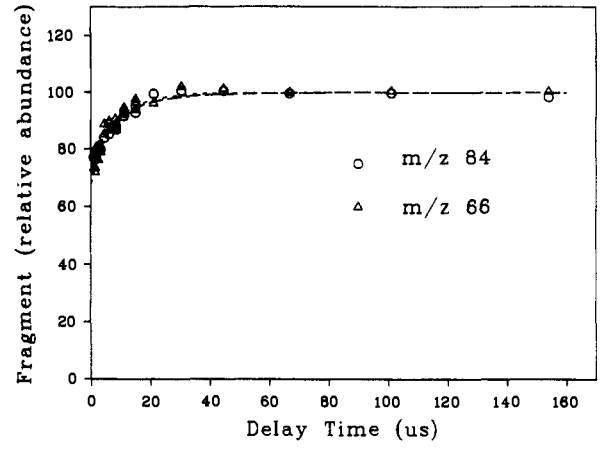

Figure 2. TRPD curve for m/z 66 and 84 photoproduction at 308 nm.

of the dissociations leading to each, but this is actually not the case. Assuming that the photoexcited parent ion branches *competitively* to the two products, the shapes of the appearance curves for both product ions are identical, and both are the same as the parent ion disappearance curve. So the rate constant derived from the shape of either of the daughter appearance curves is the parent ion disappearance rate constant, that is to say, the sum of the two constants for the competing channels. The rate constant for each individual channel is obtained by multiplying this number by the branching fraction for the channel in question.

Figure 1 shows the ICR photodissociation mass spectrum (light-on and light-off) at 308 nm, taken on the Fourier-transform ICR spectrometer. It is seen that m/z 84 and 66 are the only major photodissociation products and are produced in comparable abundance, although the branching ratio is unreliable here since the parent ions were not thoroughly thermalized in this spectrum. By using thermalized parent ions TRPD curves were obtained for both m/z 84 and 66 ions at 308 nm, as shown in Figure 2, and for m/z 84 at 355 nm, as shown in Figure 3. There was insufficient photoproduction of m/z 66 for measurement at 355 nm, and it was estimated on the basis of the detection limits of the instrument that m/z 66 production was less than 25% of m/z 84 production.

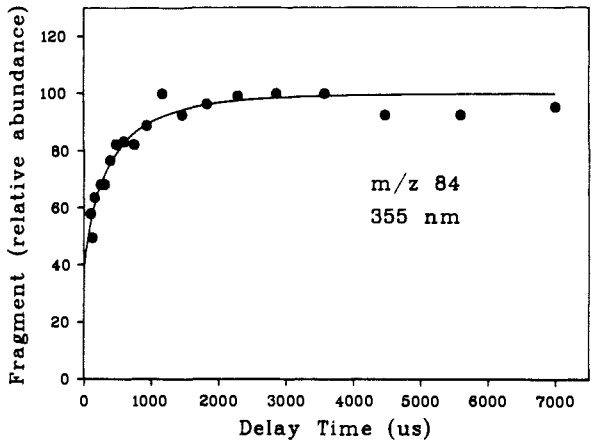

Figure 3. TRPD curve for m/z 84 photoproduction at 355 nm.

Dissociation Rate Constants. Analysis of the 308-nm TRPD curves requires care, since the dissociation rate is near the limit of time resolution of the technique. The basic signal equation is[2a]

$$S^0(\tau) = C[\Delta + (1/k)e^{-k\tau}(e^{-k\Delta} - 1)] \quad (1)$$

where $S(\tau)$ is the daughter ion signal as a function of the delay τ between the laser pulse and the beginning of the ICR excite pulse, Δ is the length of the excite pulse, and k is the dissociation rate constant. However, a correction is needed in case the dissociation is fast and the ratio of parent to daughter masses is not sufficiently large, as was particularly true for m/z 84 production at 308 nm. The correction term was derived in ref 2c and takes the form (taking $C = 1$)

$$S_{corr} = S^0 + \frac{1}{k}\frac{\omega_p}{\omega}\frac{1}{1 + (\delta/k)^2}e^{-k\tau}\left[1 - \frac{k}{\delta}e^{-k\Delta}\sin\delta\Delta - e^{-k\Delta}\cos\delta\Delta\right] \quad (2)$$

where ω_d and ω_p are the cyclotron angular frequencies of the daughter and parent ions, respectively, $\delta = \omega_d - \omega_p$, and $\omega = (\omega_d + \omega_p)/2$.

Finally, if the thermal spread of internal energies is significant, the thermal distribution of rate constants $k(E)$ must be folded into eq 2 as discussed in ref 2a:

$$S_{thermal} = \int P(E)S_{corr}(E + E_{photon})\,dE \quad (3)$$

where $P(E)$ is the probability of an ion possessing initial thermal internal energy E. This was done with use of a cell temperature of 375 K.

As expected, the photoproduction curves for m/z 66 and 84 at 308 nm had similar shapes (Figure 2), supporting the assumption that these ions are produced competitively. Equation 3 gave good fits to the curves, from which rate constants of 2.0×10^5 s^{-1} (m/z 84) and 2.2×10^5 s^{-1} (m/z 66, average of seven values) were derived at 4.20 eV internal energy. The best overall rate constant value was considered to be 2.2×10^5 s^{-1}. A branching ratio of 1.4:1 was measured for the m/z 84:66 ratio. This implies unimolecular dissociation rate constants of 1.3×10^5 s^{-1} for the m/z 84 reaction and 9×10^4 s^{-1} for the m/z 66 reaction. Equation 3 gave an excellent fit to the 355-nm data (Figure 3) with use of a rate constant of 2.8×10^3 s^{-1} at 3.66 eV. Assuming a negligible m/z 66 contribution to dissociation at this energy, this value may be taken as the unimolecular dissociation rate for the dissociation of parent ion to m/z 84. (It was estimated that m/z 84 production was at least 4 times greater than m/z 66 production at 355 nm, which sets a lower limit of 2.2×10^3 s^{-1} for the m/z 84 production rate constant, and an upper limit of 5×10^2 s^{-1} on the m/z 66 production rate constant. However, since the m/z 66 production rate is actually believed to be much smaller than this, it was neglected and no correction was made to the observed m/z 84 rate constant.) The uncertainty in the dissociation rate constants is conservatively estimated as ±10%. These rate values can be combined with RRKM modeling to draw rate–energy curves for the m/z 66 and 84 dissociation reactions, as described below.

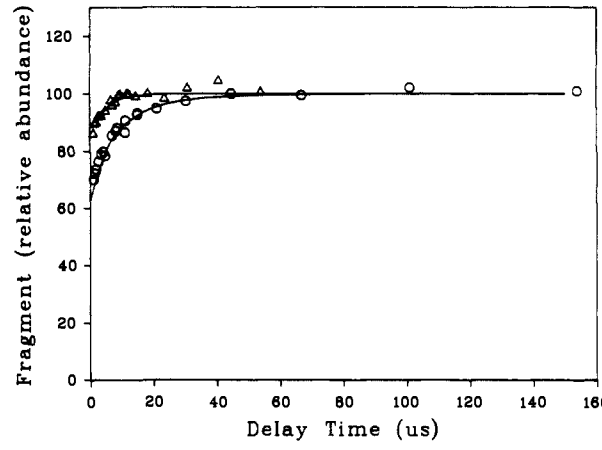

Figure 4. Comparison of TRPD curves for m/z 66 photoproduction at 308 nm with thermalized (○) and unthermalized (△) parent ions, showing the markedly faster dissociation for the ions containing excess internal energy.

Collisional Cooling and Ion Thermalization. Because the rate of photodissociation yielding m/z 66 was so much faster than initially expected, pains were taken to assure thermalization of the parent ions and to exclude the possibility of a large rate acceleration due to unrelaxed excess internal energy. As illustrated in Figure 4, electron-impact-produced ions were indeed superthermal: the figure compares TRPD curves with and without thorough thermalization. The upper set of data points were taken with the laser pulse 1 s after ionization, at a pressure of 5×10^{-8} Torr, giving one to two collisions before the laser pulse, while the lower set of points used a delay of 2 s and a pressure of 6×10^{-7} Torr, giving approximately 25 collisions. The photoappearance rate is almost 3 times faster under the low pressure conditions (6×10^5 s^{-1}) than under the higher pressure conditions (2.2×10^5 s^{-1}). As shown below, 25 collisions are in fact more than ample for thorough thermalization of the ions.

The use of TRPD in this way as an ion thermometric technique for observing ion cooling has been described several times for other ions,[2a,b] a recent study of styrene ion being particularly comprehensive.[2c] Since this approach to measuring small amounts of unrelaxed excess internal energy was both convenient and successful for thiophenol ion, a more extensive set of data was taken from which the collisional cooling rate could be estimated. The radiative cooling properties of thiophenol ion were studied in previous studies with use of two-photon photodissociation methods,[4] but the collisional cooling rate was not very well determined. Dissociation rate constants were measured as a function of the number of thermalizing collisions from 0.7 to 40. By using the rate–energy curve (shown below as Figure 6) to convert the dissociation rate constants into excess internal energy values, a curve of energy versus collision number was constructed as shown in Figure 5. While the scatter of this plot is substantial, one should note that the sensitivity of the measurement to excess internal energy is very high, with a precision of the order of 0.02 eV.

Assuming as a reasonable approximation that the initial internal energy of the ions decreases exponentially due to both collisional and infrared–radiative relaxation processes,[5] the excess ion internal energy E is expected to follow the function

$$E(t) = E_0 e^{|-(k_r + k_c P)t|} \quad (4)$$

where E_0 is the initial energy, k_r and k_c are the radiative and collisional relaxation rate constants, and P is the pressure of neutrals. Since t was constant at 1 s in this series of experiments, the radiative contribution was constant, giving

$$E(t) = (\text{constant})e^{-k_c P t} \quad (5)$$

Table I. Time-Resolved Appearance Energies by VUV Photoionization

m/z	process	AE, eV t = 20 μs	t = 150 μs	t = 800 μs
66	$C_6H_5SH \rightarrow c\text{-}C_5H_6^{\cdot+} + CS$	11.9 ± 0.1	11.85 ± 0.05	11.7 ± 0.1
84	$\rightarrow c\text{-}C_4H_4S^{\cdot+} + C_2H_2$	11.7 ± 0.1		11.5 ± 0.1
109	$\rightarrow C_6H_5S^+ + H^{\cdot}$	11.8 ± 0.1		
110	$\rightarrow C_6H_5SH^{\cdot+}$	8.3 ± 0.05		

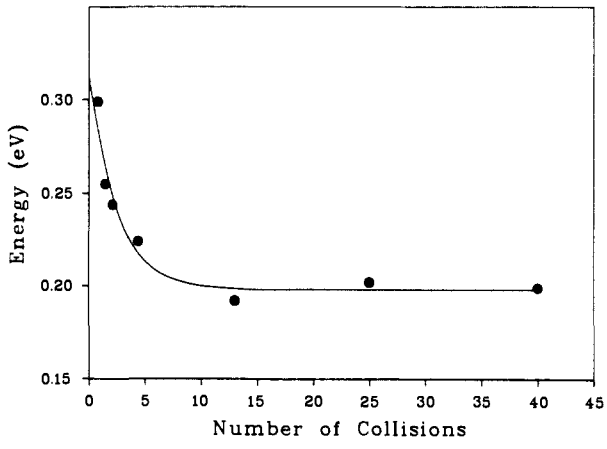

Figure 5. Internal energy of thiophenol ions as a function of pressure of neutral gas, measured 1 s after the electron beam pulse. The internal energies were measured by quantitative analysis of TRPD curves like those shown in Figure 4.

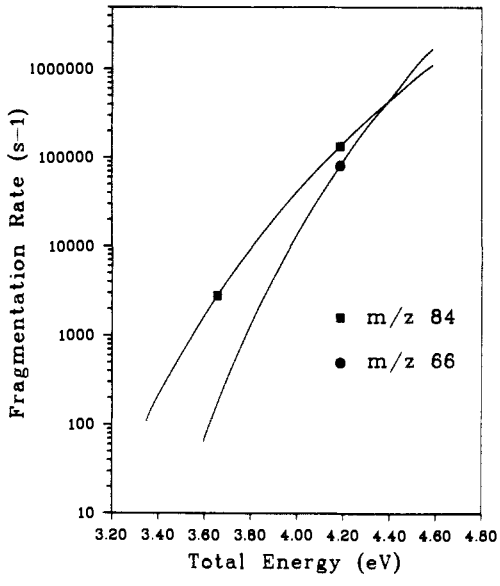

Figure 6. Rate–energy curves calculated by RRKM modeling for the two thiophenol ion dissociation channels by using the transition states and parameters described in the text. Also shown are the points for m/z 84 (■) and the point for m/z 66 (●) obtained from the TRPD results.

The exponential curve drawn through the points on Figure 5 provides an acceptable fit to this expected exponential decay.[6] The decay constant is 3 collisions, corresponding to a collisional cooling rate constant of 4×10^{-10} cm^3 molecule^{-1} s^{-1}, which indicates that two collisions remove half the excess energy in the parent ion, even when the excess energy is in the very low regime between thermal and 0.1 eV. (Given the data scatter and the uncertainty in absolute pressure determination, this value is probably uncertain within a factor of 2.) Collisional cooling is thus quite efficient.

Efficient collisional cooling of an ion by its parent neutral molecule is common in the somewhat higher internal energy regime (0.5–3 eV) for which most experimental information is available[7] and was also found for styrene ion in the low-energy regime.[2c] Resonant charge transfer is generally accepted as accounting for the high collisional cooling efficiency, and this mechanism would be expected to remain highly efficient even under the present conditions of small excess energy above thermal.

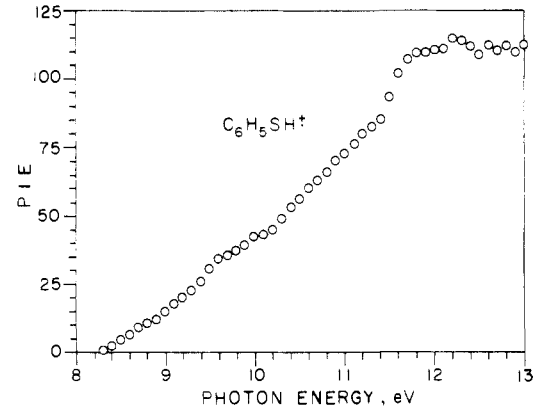

Figure 7. Photoionization efficiency (PIE) curve for the parent ion from thiophenol. The PIE (ion counts divided by light intensity, arbitrary units) is plotted versus the photon energy. Ion drawout is continuous with an ion dwell time in the ion source of ~20 μs.

Two-Photon Photodissociation. At visible wavelengths, the photodissociation of thiophenol ion is energetically inaccessible with one photon, and dissociation occurs by sequential absorption of two photons. This two-photon process was extensively characterized and exploited with use of several techniques in the ICR ion trap with the aim of measuring ion energy relaxation rates.[4] For the purposes of the present discussion, the important point is that as the photon energy approaches the one-photon dissociation threshold, a transition from two-photon kinetics is expected, signaled by changes in the pressure dependence, laser chopping rate dependence, and light intensity dependence of the extent of dissociation.

As an approach to fixing the dissociation threshold energy for thiophenol ion, the dissociation kinetics were characterized by using 458-nm (2.71 eV) photons from the argon ion laser. The kinetics showed unquestionable two-photon behavior at this wavelength. It is expected that one-photon characteristics of the kinetics would be observed if the one-photon threshold were less than 2.9–3.0 eV (allowing for the thermal energy content of the ions). Accordingly, this result was taken as a further confirmation that the dissociation threshold for thiophenol ion is not lower than 2.9 eV.

Time-Resolved Photoionization Mass Spectrometry. Photoionization (PI) mass spectrometry detected the two primary dissociation channels of the thiophenol cation radical discussed above, C_2H_2 and CS elimination, respectively, plus a hydrogen atom loss channel. All of these reactions have been observed previously,[8,9] and their appearance energies (AE's) have been determined by electron impact (EI) ionization.[8] In the PI study we concentrated on the two reactions observed under

(6) The expectation of exponential radiative cooling was discussed in: Dunbar, R. C. *J. Chem. Phys.* **1989**, *90*, 7369. While exponential collisional cooling seems to be a reasonable first approximation, there is little theory or data bearing on this question.

(7) Ahmed, M. S.; Dunbar, R. C. *J. Chem. Phys.* **1988**, *89*, 4829 and earlier references.

(8) Earnshaw, D. G.; Cook, G. L.; Dinneen, G. U. *J. Phys. Chem.* **1964**, *68*, 296.

(9) The Mass Spectra of Thiols. Lifshitz C.; Zaretskii, Z. V. In *The Chemistry of the Thiol Group*; Patai, S. Ed.; John Wiley: New York, 1974; Chapter 6.

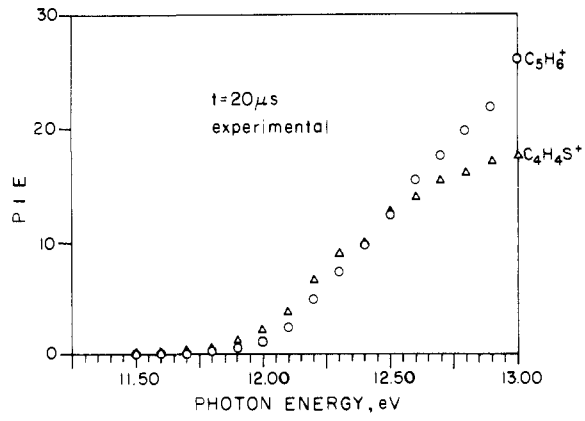

Figure 8. Experimental PIE curves for $C_4H_4S^{\bullet+}$ and $C_5H_6^{\bullet+}$ from thiophenol for t = 20 μs: (Δ) $C_4H_4S^{\bullet+}$; (○) $C_5H_6^{\bullet+}$ PIE (arbitrary units) versus photon energy, eV. The two ions are to the same scale.

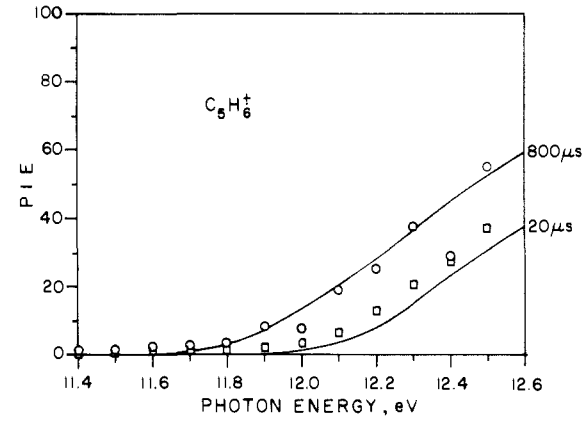

Figure 9. Time-resolved experimental ((□) 20 μs; (○) 800 μs) and calculated (—) $C_5H_6^{\bullet+}$ PIE curves; the relative intensities of the experimental PIE curves of the parent served to scale the daughter PIEs at the two storage times, without any background subtraction. The scaling factor of the calculated curve at 800 μs was calculated to give minimum standard deviations.

photodissociation—$C_4H_4S^+$ and $C_5H_6^+$ formation, with special emphasis on the latter. We have previously studied[10] by TPIMS the analogous decarbonilation reaction of phenol. In phenol the only fragmentation between 11.59 eV and about 13 eV is the loss of CO to produce the cyclopentadiene ion $C_5H_6^{\bullet+}$.[11]

Photoionization efficiency (PIE) curves were determined experimentally for t = 20 μs, for the parent ion, m/z 110, and the three primary daughter ions at m/z 84, 66, and 109, respectively. The PIE curve for the parent (Figure 7) demonstrates a sharp onset at 8.3 ± 0.05 eV in excellent agreement with the ionization energy of thiophenol.[12] It levels off at ~11.6 eV near the onset of fragmentation, as is expected for statistical RRKM-like behavior.[13] The PIE curves for $C_4H_4S^{\bullet+}$ and $C_5H_6^{\bullet+}$ are represented in Figure 8. $C_4H_4S^{\bullet+}$ is observed to have the lower onset, but $C_5H_6^{\bullet+}$ has a sharper rise and the two curves cross at ~12.5 eV. The PI appearance energies for the parent and all three daughter ions are summarized in Table I. The agreement with the EI data[8] is surprisingly good.

It should be emphasized that photodissociation is a monoenergetic technique in which all the parent ions are excited to the same energy (within the thermal spread), whereas photoionization excites parent ions to a range of internal energies extending from zero up to the maximum available energy. Therefore branching ratios and dissociation rates cannot be directly compared between the two techniques (as for instance trying to compare the branching ratios of Figures 6 and 8) but must be related to each other through appropriate theoretical modeling techniques.

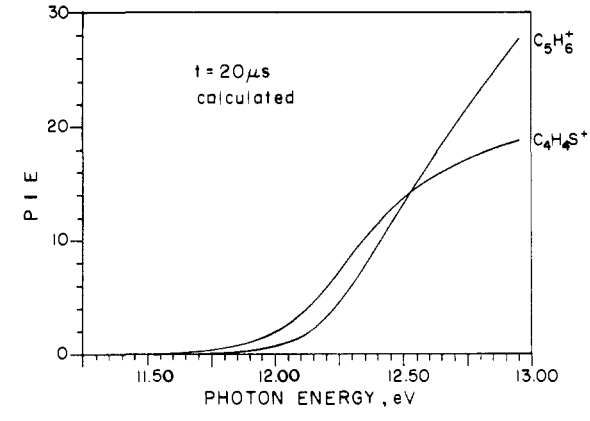

Figure 10. Calculated PIE curves for $C_4H_4S^{\bullet+}$ and $C_5H_6^{\bullet+}$ for t = 20 μs.

We next measured the PIE curves for $C_5H_6^{\bullet+}$ as a function of ion storage time. The onset regions for t = 20 and 800 μs, respectively, are represented in Figure 9. A kinetic shift of ~0.2 eV is observed. Time-resolved AE's are summarized in Table I.

PIE curves were modeled by RRKM/QET calculations employing similar models to the ones that gave agreement with the TRPD data. The microcanonical rate coefficients $k(E)$ for the two parallel reactions of $C_6H_5SH^{\bullet+}$ were calculated (the H•-loss channel was not included in the calculation). These $k(E)$ dependences were employed to calculate time-resolved parent and daughter ion breakdown curves at 0 K. Breakdown curves give the dependence of the fractional abundances of the ions on the internal energy of the parent ion. Fractional abundances were calculated from simple first-order kinetic equations. The PES (photoelectron spectrum) of thiophenol[14] was adopted as the energy deposition function for our photoionization experiments. The thermal energy distribution of the neutral molecules at the temperature of the experiment was calculated on the basis of the known vibrational frequencies of thiophenol. The 0 K breakdown curves were convoluted with the instrumental slit function, with the calculated thermal energy distribution at the temperature of the experiment, and with the PES. The resultant curves represent the calculated first derivatives of the PIE curves of the daughter ions provided the threshold law for photoionization is a step function.[13,15] These curves were integrated to compare them with time-resolved experimental PIE curves.

Calculated PIE curves for the two major parallel reactions in thiophenol at t = 20 μs are represented in Figure 10. The models employed are E_0 = 3.2 eV and $\Delta S^{\ddagger}$ = 14 eu for $C_5H_6^{\bullet+}$ and E_0 = 2.9 eV and $\Delta S^{\ddagger}$ = 2.7 eu for $C_4H_4S^{\bullet+}$. The resultant curves are in excellent agreement with the experimental ones (Figure 8). Furthermore, the model reproduces rather well (Figure 9) the relatively small kinetic shift for $C_5H_6^{\bullet+}$ between 20 and 800 μs.

MIKES. The MIKE spectrum of the parent ion demonstrated three metastable transitions: H• loss (m/z 109), CS elimination (m/z 84), and C_2H_2 elimination (m/z 66) and a very small contribution from m/z 108. Kinetic energy releases (KERs) were determined for the peaks at m/z 66 and 84, respectively. The peak at m/z 66 ($C_5H_6^{\bullet+}$) is a narrow Gaussian with $T_{1/2}$ = 20 ± 2 meV. It was analyzed by the method of Holmes et al.,[16,17]

(10) Malinovich, Y.; Lifshitz, C. *J. Phys. Chem.* **1986**, *90*, 4311.
(11) Fraser-Monteiro, M. L.; Fraser-Monteiro, L.; de Wit, Jos; Baer, T. *J. Phys. Chem.* **1984**, *88*, 3622.
(12) Rosenstock, H. M.; Draxl, K.; Steiner, B. W.; Herron, J. T. *J. Phys. Chem. Ref. Data* **1977**, *6*, Suppl. 1. Lias, S. G; Bartmess, J. E.; Liebman, J. F.; Holmes, J. L.; Levin, R. D.; Mallard, W. G. *J. Phys. Chem. Ref. Data* **1988**, *17*, Suppl. 1.
(13) Chupka, W. A. *J. Chem. Phys.* **1959**, *30*, 191.
(14) Kimura, K.; Katsumata, S.; Achiba, Y.; Yamazaki, T.; Iwata, S. *Handbook of HE I Photoelectron Spectra of Fundamental Organic Molecules*; Japan Scientific Societies Press, 1981; p 193.
(15) Chupka, W. A.; Berkowitz, J. *J. Chem. Phys.* **1967**, *47*, 2921.
(16) Holmes, J. L.; Terlouw, J. K. *Org. Mass Spectrom.* **1980**, *15*, 383, Table 2.

and the average kinetic energy release was found to be $\langle T \rangle = 52 \pm 5$ meV. The peak at m/z 84 ($C_4H_4S^{+}$) is considerably broader with $T_{1/2} = 110 \pm 10$ meV and not quite Gaussian-type. The kinetic energy release distribution was obtained from the first derivative of the metastable ion peak shape,[18] and this led to $\langle T \rangle = 151 \pm 5$ meV. The higher KER observed for the C_2H_2 elimination is in agreement with its lower threshold energy compared to the CS loss. A small reverse activation energy (<0.1 eV) cannot be ruled out, however, and is in agreement with the reaction having a somewhat tighter transition state.

CA MIKES. The structure of the m/z 84 ion was studied by MIKES and by collisional activation (CA). The MIKE spectrum demonstrated H loss, H_2 loss, and a strong C_2H_2 loss peak. The CA spectrum demonstrated additional peaks at m/z 81, 69, 57, 51, 50, 45, 39, 38, 37, 27, and 26 with 45 and 39 being particularly intense. The MIKES and CA spectra were equal in every detail with those of the parent ion from thiophene, indicating that $C_4H_4S^{+}$ from thiophenol has the thiophene cation radical structure.

Discussion

The initial motivation for the careful study of thiophenol ion rate–energy curves reported here was the surprising observation that the m/z 66 photodissociation was much faster than expected on the basis of the expected tight transition state and with the accepted threshold of 3.2 eV. It has become clear that this observation is correct and that a loose transition state is inescapably necessary for RRKM modeling of this reaction. To clarify this question, calculations were done with use of a reasonably tight transition state having a calculated $\Delta S^{\ddagger}(1000\ K)$ of −1.4 eu. By using a critical energy of 3.2 eV, this leads to a calculated dissociation rate of $6 \times 10^2\ s^{-1}$ at 4.22 eV internal energy (corresponding to photodissociation at 308 nm), nearly 100 times slower than the observed rate at 308 nm. Thus, such a model is completely unsuccessful.

A more serious possibility is that the transition state is tight, but the activation energy for this dissociation is lower than 3.2 eV. By using the same tight transition state and a critical energy of 2.9 eV, a rate–energy curve can be calculated which gives a roughly correct rate of $5 \times 10^4\ s^{-1}$ at 4.2 eV. There are, however, a number of reasons to reject this model for the dissociation. The first difficulty with this model is its divergence from experiment at lower internal energies. At 3.66 eV, corresponding to 355-nm photodissociation, the rate is predicted to be $2 \times 10^3\ s^{-1}$ while, as seen above, the TRPD results at 355 nm put an upper limit of $5 \times 10^2\ s^{-1}$ for the dissociation to m/z 66. Along the same lines, this model clearly predicts that m/z 66 will be comparable to m/z 84 at low internal energies, while both the TRPD result at 355 nm and the TPIMS curves clearly show that m/z 84 is the dominant dissociation product at low internal energies. Moreover, an activation energy of 2.9 eV for m/z 66 production is hard to reconcile with the convincing threshold observed near 3.2 eV in the 2-ms TPIMS curve. And finally, the dissociation endothermicity of 3.2 eV which is calculated from rather good thermochemical values[12] is probably near the activation energy for dissociation. Accordingly, such a tight transition state may be totally ruled out for this dissociation within the assumption of the applicability of RRKM theory. Since we would assume RRKM theory to be valid unless forced to abandon it, we will discuss this reaction further on the assumption that the rate-limiting transition state is indeed fairly loose, with $\Delta S^{\ddagger}(1000\ K) = +14$ eu.

By using this loose transition state with a critical energy of 3.2 eV, the rate–energy curve shown in Figure 6 is calculated for m/z 66 formation. As noted on the plot, this curve passes through the TRPD point determined at 308 nm. It was also used as the basis for the satisfactory modeling of the TPIMS results described above.

The rate–energy curve for m/z 84 formation shown in Figure 6 is obtained by using a somewhat tight transition state, with

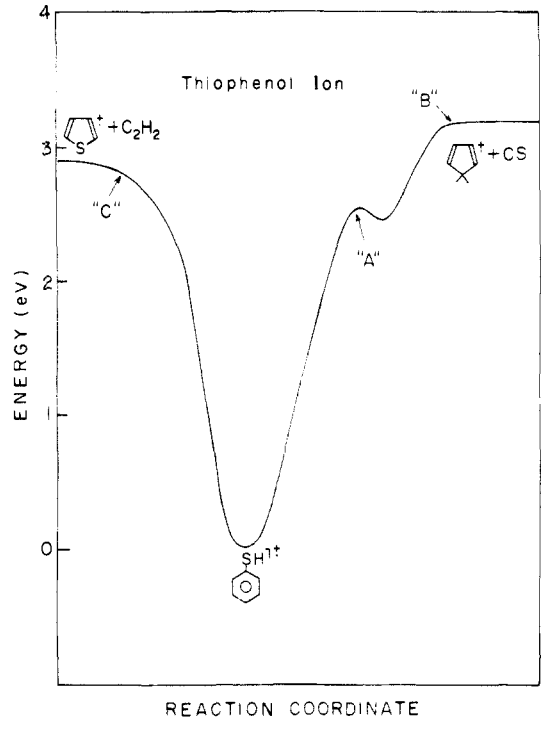

Figure 11. Proposed potential energy surface for the two dissociation channels for thiophenol ion.

$\Delta S^{\ddagger}(1000\ K) = 2.74$ eu and critical energy of 2.82 eV. As shown, it passes through the two TRPD points; it was also successful in modeling the TPIMS curves. This transition state, which is much tighter than an orbiting transition state, does not seem unreasonable for a rearrangement dissociation. The endothermicity of the m/z 84 dissociation, assuming a product ion of the thiophene structure, is calculated from thermochemical values[12] as 2.91 eV. Thus the critical energy (2.82 eV) derived from the RRKM fit is slightly lower than the endothermicity, which is not unreasonable for a tight transition state (although this energy difference may not be experimentally significant).

Potential Surface Model. The potential surface proposed to account for the loose transition state in the rate-limiting step of the m/z 66 reaction is sketched in Figure 11. It is suggested that the tight transition state corresponding to the molecular rearrangement, designated "A" on the figure, has negative activation entropy, but it has an energy below 2.9 eV, so that passage through this transition state is not rate limiting in the internal energy regime of interest here. The rate-limiting loose transition state, designated "B", has an energy of 3.2 eV and a $\Delta S^{\ddagger}$ of +14 eu, which are the kinetic parameters indicated by the data for the rate-limiting step.

The nature and structures of these transition states can only be pure speculation, but to clarify thinking about them, we can speculate that the dissociation mechanism might look like that shown in Scheme I, assuming a 1,3-hydrogen shift rearrangement route for the sake of argument.

The breaking of the C–C bond in transition state "B" is suggested as the high-energy process on the potential surface, so that even though its entropy is high, approaching the looseness of an orbiting transition state, nevertheless it constitutes the kinetic bottleneck in the dissociation.

It should be emphasized that the two-transition-state picture of this dissociation is proposed as being strongly implied by the experiments, but without any serious advocacy of the particular speculative transition-state structures drawn in Scheme I. One possibly testable prediction of this model is that the m/z 66 dissociation process should exhibit transition-state switching at some internal energy above 4.2 eV, as the tight transition state becomes rate limiting and slows the dissociation below the rate suggested by extrapolating the rate–energy curve of Figure 6 to

(17) Holmes, J. L.; Osborne, A. D. *Org. Mass Spectrom.* **1981**, *16*, 236.
(18) Holmes, J. L.; Osborne, A. D. *Int. J. Mass Spectrom. Ion Phys.* **1977**, *23*, 189. Jarrold, M. F.; Wagner-Redeker, W.; Illies, A. J.; Kirchner, N. J.; Bowers, M. T. *Int. J. Mass Spectrom. Ion Processes* **1984**, *58*, 63.

Scheme I. Speculative Structures Along the Reaction Coordinate for m/z 66 Formation

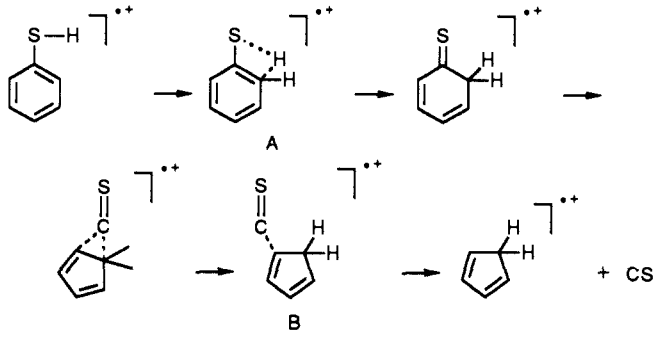

higher energies.[19]

Kinetic Energy Release. The very low kinetic energy release of $T_{1/2}$ = 20 meV, $\langle T \rangle$ = 52 meV for m/z 66 formation fits with the very loose, near-orbiting transition state assigned to this channel. Since the critical energy assigned to the m/z 84 formation channel is near or below the reaction endothermicity, a significant reverse activation energy for this channel seems unlikely. Therefore, the higher kinetic energy release of $T_{1/2}$ = 110 meV, $\langle T \rangle$ = 151 meV measured for this channel can be attributed to energy partitioning into translation in the somewhat tight transition state.

Comparison with Phenol. An interesting comparison and contrast with the corresponding dissociation of phenol ion can be made. The activation energy for CO loss from phenol ion is about 2.9 eV,[10,11] which is notably in the same vicinity as the suggested upper limit for the speculative rearrangement transition state "A" in the thiophenol case. However, phenol is very different in that the dissociation endothermicity (about 1.3 eV) is much less than the activation energy, so that phenol ion exhibits a large reverse activation energy for this process, accompanied by a large kinetic energy release. Thus we might draw a corresponding potential surface for phenol ion dissociation as in Figure 12.

For neutral systems, the special stability of CO is such that extracting CO from an alcohol is of the order of 2 eV less endothermic than extracting CS from the corresponding thiol. In the case of phenol and thiophenol ions, it is similarly true that the loss of CO from phenol ion is about 2 eV less endothermic than loss of CS from thiophenol ion (1.3 vs 3.2 eV). Assuming that this added product stabilization in the alcohol case develops as the carbon rehybridizes to form the triple bond of CO, it is entirely reasonable that the rearrangement transition state "A" in Figure 11 would have similar energies in the phenol and thiophenol cases; but in the phenol case the dissociation would be strongly downhill from this point, while in the thiophenol case it would be uphill, with the second transition state "B" turning out to be rate determining. These contrasting pictures are clearly seen in the comparison of Figures 11 and 12. Thus, as we view it, for phenol ion the rearrangement transition state is rate limiting, while for thiophenol ion the orbiting transition state corresponding to separation of the products is rate limiting, with the prior rearrangement being kinetically insignificant.

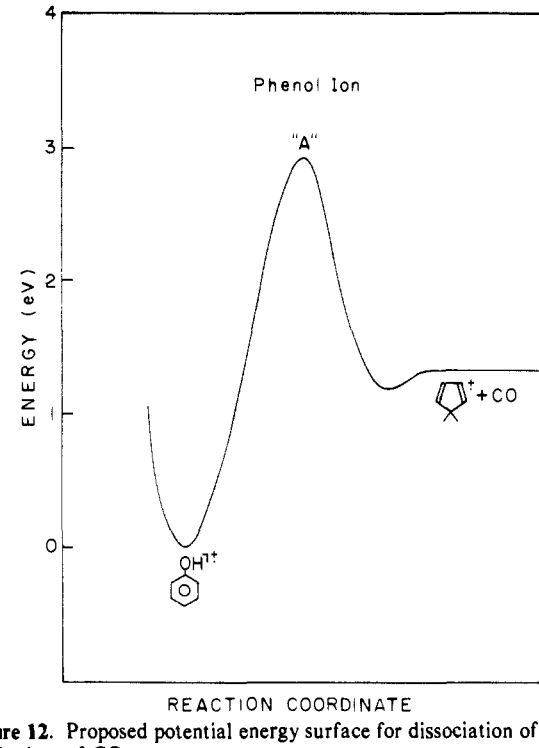

Figure 12. Proposed potential energy surface for dissociation of phenol ion by loss of CO.

Acknowledgment. This research was partly supported by a grant from the United States-Israel Binational Science Foundation (BSF), Jerusalem, by the U.S. National Science Foundation, and by the donors of the Petroleum Research Fund, administered by the American Chemical Society.

(19) The potential surface, particularly for the loss-of-acetylene channel, is undoubtedly much more complex than the simple curves of this diagram. Since we have no information on features of the potential surface other than rate-limiting transition states, we have not attempted speculation on further features not discussed here. High-level quantum chemical calculation is probably the best approach to mapping further details of the surface. While a tight transition state (or more than one) for ion rearrangement prior to CS loss undoubtedly exists (for which the structure designated "A" is a speculative possibility), we have no experimental information about this state or states. The calculation mentioned in the text, showing that such a state would become rate-limiting with $\Delta S^{\ddagger} = -1.4$ and $E_0 > 2.9$ eV, serves as an example of the constraints on the kinetic parameters imposed by requiring passage through this state to be fast compared with the dissociation rate. However, beyond suggesting that the energy of such a state is probably not much above 2.9 eV, there is no more we can say about the properties of such kinetically invisible states.